Electron-induced decomposition and time-dependent breakdown of ionic solids: An experimental study on silver azide

Tong B. Tang* and M. Munawar Chaudhri
Cavendish Laboratory, Madingley Road, Cambridge CB3 OHE, United Kingdom
(Received 12 April 1984)

An experimental study has been made of the time-dependent dc electrical breakdown of single crystals of silver azide (AgN_3), an exothermic ionic solid which reacts chemically in an explosive manner after the breakdown. The lowest breakdown field at room temperature was 13 kV/m, which is some 4 orders of magnitude smaller than that for most other ionic solids. Moreover, the time delay to breakdown may be up to several days. The study consisted of several series of experiments, namely (i) the behavior of the current conducted through the sample under different applied fields, (ii) optical and electron microscopies of the test crystal during the period leading up to the breakdown, (iii) mass spectrometry of the gaseous products evolved during the breakdown process, (iv) the response of the crystal to ac fields of different frequencies and magnitudes, (v) the effect of having only one conducting contact on the crystal, and (vi) the identification of the locations of the sites in the crystal where dielectric breakdown initiated. The experiments established that the breakdown of a test crystal occurred only if, at a sufficiently high applied dc field, the current conducted through it developed instabilities; during these instabilities the crystal suffered chemical reaction as evidenced by the appearance of isolated globules of metallic silver on the surface and by the evolution of nitrogen gas. The breakdown and the consequent initiation of an explosion generally occurred at regions away from the electrodes. Based on these observations it is suggested that the instabilities occur due to the double injection of electrons and holes into the silver azide crystal from the cathode and anode, respectively; the injection of charge carriers gives rise to the chemical reaction of the crystal. The injection is thought to occur due to the presence of high interfacial fields because of electrode polarization, which, in turn, is caused by the drift of interstitial Ag^+ ions under the action of a dc field applied through partially blocking electrodes. It is also proposed that our model may be applicable to other ionic solids, for example, the β-aluminas and CdF_2.

I. INTRODUCTION

There is as yet no unambiguous model for the breakdown of insulation in ionic solids.[1] With the aim of understanding this phenomenon we have carried out an experimental study on silver azide, AgN_3, which serves as a prototype for all ionic materials that decompose exothermically.[2]

Silver azide is a sensitive and powerful solid explosive which is used extensively as a detonant. Although much research has been done on its explosive properties, certain aspects of its behavior are still far from being clearly understood. One such aspect is the initiation of explosion by dielectric breakdown after long delay times at low dc fields. In this paper we discuss the results of our investigation of silver azide's reactivity during the passage of an electric current too small to cause thermal decomposition. An explanation of the underlying mechanisms is put forward which is consistent with experimental observations.

The fact that silver azide can decompose exothermically into silver and nitrogen gas under the action of many kinds of stimuli is well known. The decomposition may be slow and controlled if the strength of the stimulus is low. Alternatively, it may become fast and self-sustained once, within a sufficiently large region and for a sufficiently long time,[3] the rate of heat evolution due to the reaction exceeds the rate of heat loss. In the latter, the fast decomposition will propagate through the entire volume of the azide at a speed of 1 to 3 km/s, resulting in an explosion. This reaction velocity is 6—7 orders of magnitude greater than that of slow decomposition: It is because of the dramatic decrease of time scale that explosions in themselves are difficult to study in detail. On the other hand, the processes leading to their initiation after the application of a stimulus may, in the case of an electrical stimulus, take as long as several days. These processes constitute the subject of the present investigation.

Explosion initiation of AgN_3 single crystals by dielectric breakdown was first noted by Bowden and McLaren[4] of the Cavendish Laboratory, Cambridge, United Kingdom. Explosions were reported to occur in crystals of dimensions $1.0\times0.5\times0.5$ mm^3 when about 45 V dc was applied across them and the conduction current had subsequently risen to roughly 150 μA. The corresponding current density, calculated on the assumption of uniform flow, was too small to cause any significant Joule heating, and, therefore, a different explanation was sought. Bowden and McLaren proposed that (1) the azide was an *n*-type semiconductor, so that, with a voltage across the crystal, a space charge of immobile positive holes accumulated in front of the cathode, and (2) at a sufficiently high applied voltage the space-charge field became sufficiently intense to induce field injection of electrons, which, in turn, led to impact ionization, chemical decomposition, self-heating, and finally to initiation of an explosion. This model needs drastic modifications, as was

shown by subsequent work, and as is shown in this paper. Subsequent measurements of the thermoelectric power by Young[5] and of the conductivity of doped material by Zakharov *et al.*[6] have shown that the principal current carriers are not free electrons but interstitial cations. Moreover, there is a major discrepancy: The model predicts that explosions always are initiated adjacent to the cathode, whereas observations reported in this paper indicate that the point of initiation is generally somewhere else. Nevertheless, the original report served to bring the phenomenon to the attention of research groups in the United States and the Soviet Union, who then also studied several other azides. Their results regarding the various breakdown fields together with respective electrical conductivities are listed in Table I.

It may be seen in the table that, with the exception of cuprous azide, which has complex conductance characteristics,[8] silver azide has the lowest breakdown-field strength, followed by thallous and lead azides. This is surprising since, in any other aspect, copper and mercury azides are less stable, because of their covalent nature, than the three just named, which are essentially ionic. Our investigation has concentrated on AgN_3, the easiest azide to study, although some experiments have also been carried out on TlN_3 and $Pb(N_3)_2$. Based on this work we propose a novel breakdown mechanism to explain the remarkable behavior of these ionic compounds.

In addition to the relative magnitude of breakdown field strength, another aspect of its behavior is likewise strongly suggestive of an unusual mechanism. Dielectric breakdown occurs in silver azide at still lower fields than the 1-s, 50% value given in Table I, provided these fields have been maintained for long periods of time. Moreover, corresponding to a given field, the periods exhibit a statistical distribution. Such a breakdown process at room temperature with extended and variable induction periods, during which reversible current instabilities occur, is striking, but apparently has received little attention before. Preliminary observations point to a similar long-term effect of low fields in thallous and lead azides as well as in sodium azide. According to our explanation the breakdown is attributed to the chemical effects, i.e., slow decomposition, arising from injected electrons. However, these effects are not thought to be due to impact ionization in the vicinity of the cathode as proposed by Bowden and McLaren. The decomposition may occur at sites throughout the length of the crystal and can proceed for a long time before resulting in breakdown. Based on observations from experiments on other materials, we argue that this type of electrochemical breakdown may be found in many classes of ionic materials. A brief examination of the wider implication of our hypothesis will be presented in Sec. VI.

II. TYPICAL CURRENT BEHAVIOR

The room-temperature dc electrical characteristics of AgN_3 exhibit pronounced field dependence, and, therefore, for purposes of clarity, we begin with a classification of the different regimes. These regimes are illustrated by the current traces shown in Fig. 1. For low applied fields the current decays slowly with time to a steady value. An example is shown by trace *a*; in this case the bulk mean value of the field is 3.3 kV/m and the electrodes are tantalum sheets. We attribute such a decay to ionic polarization at the electrodes, which are partially blocking electrodes. The steady-state value of the current has an Ohmic relationship with the value of the bulk mean field. At medium fields of 13 kV/m or more the current is no longer Ohmic but displays fluctuations, as shown by trace *b*. If the field is maintained, then after several hours or even days it will start to rise with time until dielectric breakdown and an explosion occur.

At strong fields exceeding 65 kV/m (400 and 800 kV/m for thallous and lead azides, respectively), current fluctuations of a relatively large amplitude appear immediately (see trace *c*). The value of the current averaged over each oscillation increases with time and the rate of increase of the current is greater for a higher applied field.

Another interesting observation is that if a strong field is applied to a crystal for a certain length of time and then removed for a few minutes before its second application, the rate of increase of the conduction current is higher than in the first application. We shall refer to this phenomenon as "memory effect." This effect is more

TABLE I. dc room-temperature breakdown-field strengths of a number of ionic and covalent azides.

Material	Type of bonding	Room-temperature low-field conductivity (S/m)	Breakdown-field strength[a] (MV/m)	Reference
AgN_3	ionic	3×10^{-7}	0.4[b]	present work
TlN_3	ionic	1×10^{-10}	1.2[b]	present work
			1.1[c], 1.4[c], 1.5[c]	7
α-$Pb(N_3)_2$	ionic	1×10^{-11}	1.8[a]	present work
CuN_3	complex	not known	$\approx$0.2	8
$Cu(N_3)_2$	covalent	not known	38[c], 50[c], 68[c]	7
$Hg(N_3)_2$	covalent	6×10^{-9}	several tens	8
$Hg_2(N_3)_2$	covalent	"low"	"very high"	8

[a]Field value for a 50% probability of breakdown within 1 s of its application.
[b]Needle-shaped crystal with Ag electrodes.
[c]Pellet-shaped sample with both electrodes of Zn, Cu, and W, respectively.

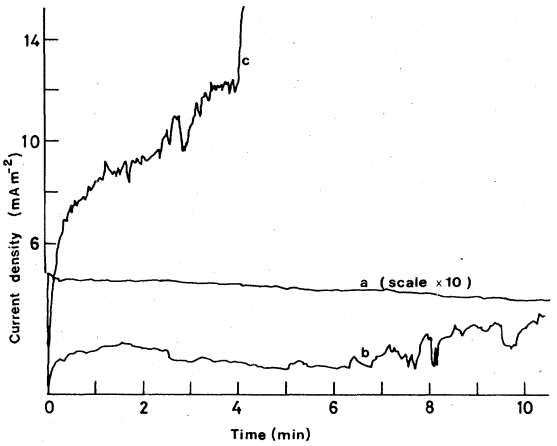

FIG. 1. Current-versus-time curves of a silver azide single crystal in ultrahigh vacuum, when dc fields of various strengths are applied along the c axis through pressure-contacted tantalum-foil springs. The dc fields for traces a, b, and c are 3.3, 13, and 67 kV/m, respectively. Qualitatively the same behavior is observed with silver and graphite electrodes.

pronounced if the time interval between the two applications of the field is shorter; the same is true if during the first application the final magnitude of the current reached is higher. Nevertheless, when several applications of the same field were made to a crystal, the magnitude of the current at the instant of the second or a later application is the same. This is also the case if a field of the same magnitude but opposite polarity is applied. It was also found that for a typical silver azide single crystal of size 10 mm$\times$100 μm $\times$100 μm the conduction current is invariably about 100 μA at the instant of the explosion initiation, as measured with a transient digital recorder (Data Lab model 922). Figure 2 illustrates a typical case.

III. EXPERIMENTAL PROCEDURE

As a result of a close study of the typical current behavior described in the preceding section, it was thought that the breakdown might be related to the development of current fluctuations at medium to strong dc fields. It was therefore decided to examine if any physical changes on the crystal surface and chemical reactions in the material occurred when the conduction current was of a fluctuating nature. In a parallel series of experiments the effects of ac fields of different frequencies were also monitored. Another series was conducted to locate the sites of explosion initiation following the dielectric breakdown. Finally, experiments were carried out to investigate the effects of intensely high fields when applied through one conducting electrode only. The results of the last two series of experiments were of particular relevance in elucidating the most likely mechanism leading to the dielectric breakdown. The various experimental arrangements, procedures adopted, and methods of analyzing data are discussed below.

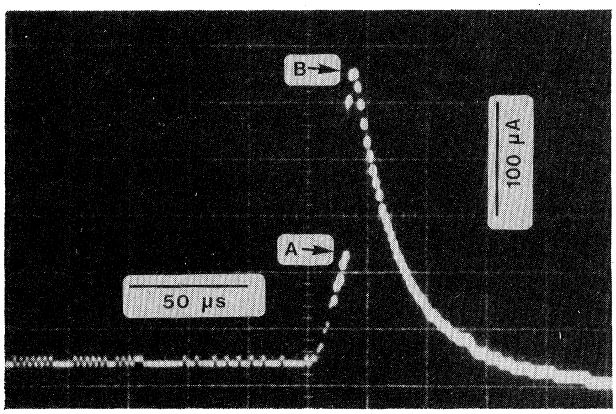

FIG. 2. Current-time behavior of a silver azide single crystal suffering dielectric breakdown. The breakdown at A is followed by an explosion at B. The decaying current is through the plasma constituted by the explosion products.

A. Microscopies

Single crystals of silver azide were grown by recrystallization from solution in ammonia.[2] The crystals were needle shaped with the c axis along the length; they were 100–300 μm thick and up to 20 mm long. The major metallic impurity was determined by atomic absorption to be iron [(70$\pm$20) ppm]. Crystals of good quality were chosen for the experiments. A crystal was placed on a glass microscope slide and electrical contacts were made at its ends with either silver dag or carbon dag; the dag also helped to hold it in position on the slide. After the electrodes were thoroughly dried in an evacuated dessicator, either a dc or an ac field was applied, with a nanoammeter and a 5.5-MΩ current-limiting resistor in series. The crystal was observed *in situ* through an optical microscope in both transmission and reflection modes, and then, when deemed appropriate, further examined in a scanning electron microscope (SEM) (Cambridge model S4-10). If any surface formations were detected, then a transmission-electron-microscope (TEM) grid having a carbon film was lightly pressed against it, so that some of the formations were transferred to the film, which could be analyzed in the SEM incorporating an energy-dispersive x-ray spectrometer (Link System model 290 with Kever model 3201 detector).

B. Mass spectrometry

Gases evolved from a AgN_3 crystal due to reactivity, under certain circumstances as specified in Sec. IV, were identified and measured in an ultrahigh-vacuum system within which a mass spectrometer was incorporated. The heart of the system was a six-way chamber consisting of tubes having Conflat model FC-38 (Vacuum Generators) flanges and welded orthogonally to one another. One horizontal arm led to a quadrupole spectrometer (Varian Associates residual gas analyzer model 974-2), to another was attached an ionization pressure gauge (head, Vacuum Generators model VIG 10; controller, model IGP 2), while the third was connected through valves to a molecular adsorption pump, a sputter-ion pump, and a nitrogen-gas bottle (British Oxygen, spectroscopically pure grade) in parallel. The bottom arm contained an electrical

feedthrough. The top and the remaining horizontal ports had glass windows for visual observation. A high-current switching circuit was inserted into the power line to the spectrometer controller. The circuit was triggered by the over pressure relay in the IGP 2 gauge controller, the set trip level of which was usually adjusted at 1.5×10^{-5} Torr. This arrangement prevented accidental damage to the electron multiplier of the spectrometer because of excessive ambient pressure due to the explosion of the test crystal.

The sample under study was placed on a thin fused-quartz plate, which, in turn, was supported on two of the feedthrough's pins. Electrical contacts between the crystal and these pins were made with springs of tantalum foil pressed onto the crystal's two ends; the contact pressure was sufficient to ensure Ohmic characteristics but not too high to cause any physical damage to the crystal. For the purpose of eliminating electrostatic interference between the circuit and the mass spectrometer, a fine copper gauge covered the porthole to which the spectrometer was connected. The total volume of the assembly was estimated to be about 1 l.

The experimental procedure was as follows: With the crystal in place, the system was pumped down to 10^{-7} Torr. Degassing of the system was then carried out by baking it several times with heating tapes; precautions were taken to avoid excessive heating of the sample region. Each baking lasted about 4 h, and toward the end of each period the filament of the spectrometer was also degassed. In this manner a pressure of 5×10^{-9} Torr was obtained in the system.

Two alternative methods were adopted to monitor any chemical changes in the crystal upon the application of a dc voltage which was sufficient to give rise to a fluctuating current. In the first method, the experimental chamber was isolated from the ion pump, and mass scans were taken of the residual gases. Owing to desorption from the chamber walls and filament, the background pressure increased slowly. A chosen voltage was then applied to the crystal. It was observed that under this condition additional pressure increase occurred which could be entirely attributed to a rise of the peak at 28 amu. We identified this rise in pressure as being due to the generation of nitrogen from the crystal. In subsequent runs, the partial pressure of nitrogen was measured in place of the total pressure. It was found that the parts of the partial-pressure—versus—time curve before and after the voltage application were linear and parallel to each other. This feature showed that upon removal of the voltage the generation of nitrogen ceased virtually immediately (on the time scale of, say, 0.1 s, corresponding to the time resolution of the measurement). In addition, during the entire experimental run when the chamber was isolated from the pump, the net rate of rise of the background pressure was essentially constant, quite independent of the base pressure. It should therefore be eliminated through extrapolation of the part of the curve before voltage application. The rate of nitrogen production by the crystal, $d(t)$, in number of molecules per unit time, could be simply calculated from the true pressure increase via the ideal-gas law.

There was a drawback in the above procedure, namely, that in a few minutes the accumulative rise of pressure reached values at which the mass spectrometer could not function properly. For the purpose of lengthening the time over which observations could be made, another method of measurement was adopted: The system was only partially isolated from the pump so that a steady pressure of $(1-5)\times10^{-8}$ Torr was maintained. The voltage was then applied and again the variation of ion-current intensity at 28 amu was followed. The procedure for data analysis to derive the rate of nitrogen evolution is described below.

Considering all the sources and sinks of nitrogen in the sample chamber, we denote the number of nitrogen molecules contained therein by N and write its rate of change as

$$\dot{N}=B+d(t)-P(t)\dot{v}/kT\ , \tag{1}$$

where B is the net rate of background evolution, assumed to be a constant throughout, $\dot{v}$ is the volumetric flow speed of nitrogen pumped through the partially closed valve, $P(t)$ is the nitrogen partial pressure in the chamber, T is the absolute temperature, and k is Boltzman's constant. Before the voltage is applied to the crystal a steady-state partial pressure $P(0)$ holds. Thus, from Eq. (1),

$$B=P(0)\dot{v}/kT\ . \tag{2}$$

Substituting this back into Eq. (1) and $p\equiv p(t)$ for $P(t)-P(0)$, which is the measured pressure increase, we obtain

$$\dot{N}=d(t)-p\dot{v}/kT\ . \tag{3}$$

Since $pV=kT[N(t)-N(0)]$, in which V is the volume of the chamber, the last equation becomes

$$\frac{dp}{dt}=d(t)kT/V-p\dot{v}/V\ . \tag{4}$$

For the case at hand, $\dot{v}$ may be taken as a constant, so that, defining $\tau\equiv V/\dot{v}$, we obtain

$$p=\frac{kT}{V}\exp\left[-\frac{t}{\tau}\right]\int_0^t d(t)\exp\left[\frac{t}{\tau}\right]dt\ . \tag{5}$$

If $d(t)$ equals a constant D between $t=0$ and $t=t^*$, but is zero afterwards, then for $t\le t^*$ Eq. (5) gives

$$p=\frac{kT\tau}{V}D\left[1-\exp\left[\frac{-t}{\tau}\right]\right]\ , \tag{6}$$

and for $t\ge t^*+t'$, $t'\ge0$,

$$p=p(t^*)\exp\left[-\frac{t'}{\tau}\right]\ . \tag{7}$$

T and V are known quantities. Equation (7) may be used to determine τ corresponding to a particular opening of the valve. This value of τ can then be substituted into Eq. (6) for the calculation of D. Often, D is constant over a period which is long compared to τ: In such a case, Eq. (6) reduces to the simple form of $p\approx p(t^*)=(kT/V)\tau D$ at sufficiently long times, when p reaches a steady-state value inversely proportional to the pumping speed. In-

cidentally, it may be noted that the sensitivity of p to D is $kT\tau/V$, whereas the response speed is $1/\tau$. Hence the "gain-bandwidth" product is kT/V. As expected, a smaller V and a higher T are advantageous, although in practice T is room temperature and not easily modified.

C. Memory effect

A "memory effect" in current behavior has been mentioned in Sec. II. To study this effect further we examined the reactivity of a crystal under repeated applications of the same electric field. The rate of nitrogen evolution was monitored with the help of the mass-spectrometric system during the first and subsequent applications, and the results were compared.

D. Location of fast-decomposition initiation

If an explosion is caused in a crystal mounted on a microscope slide, a residue in the form of fine silver particles remains on the slide after the fast decomposition has propagated from the point of initiation to other parts of the crystal. A number of specimens was exploded, with initiation points at predetermined positions, by either irradiation with a Q-switched ruby-laser beam (1 J, 20 ns) through two 200-μm slits arranged 4 mm apart over the crystal, or by a point contact with a fine copper wire through which a high-current pulse was passed to heat it to high temperatures. An examination of the residues revealed a consistent geometrical pattern; the pattern clearly indicated the positions of the initiation sites. The information formed the basis of a method for identifying the locations of initiation sites in the dielectric breakdown experiments. Accordingly, a number of crystals were subjected to electric fields between 180 and 430 kV/m, and the initiation sites were determined in this manner.

In a separate series of experiments, a 10-kV pulse of 0.5 μs rise time was applied to samples held between electrodes that were 1 mm apart. In this case it was found that the explosion always initiated within 0.2 μs of the voltage reaching its maximum amplitude. Since the propagation of an explosion through the sample would take about 1 μs, synchronization provided by the voltage pulse enabled us to record the sequence of events with high-speed photography. For this purpose an image-converter camera (Imacon model 600) was used, operated to give an interframe time of 0.2 μs. The samples were immersed in transformer oil, necessary to prevent corona discharges. The subject was backlit using the flash from a Thorn xenon-filled model FA 5 tube.

E. High-field experiment on sample with one electrode in contact

The aim of this investigation was to clarify whether the flow of a conduction current through the crystal is required for the breakdown, or if the presence of an intense electric field alone suffices. For this purpose, two polytetrafluoroethaline (PTFE) (an insulating polymer) disks 20 mm in diameter and 4 mm thick were mounted parallel to each other, with a gap of 3.3 mm between them, on a block of polymethylmethacrylate (PMMA) (another insulating polymer). In each disk a brass cylinder 6 mm in diameter was fitted along the disk's axis; the entire assembly is shown schematically in Fig. 3. The brass cylinders, across which a Brandenburg 60-kV power supply was connected, acted as electrodes, and in the center of one of them an axial hole about 0.5 mm in diameter and 1 mm deep was made. The test crystal was held in the hole with silver dag and it was ensured that, before the dag hardened, the crystal was perpendicular to the face of the cylinder. Further drying of the dag proceeded with the cylinder placed in an evacuated dessicator. The assembly was then completed. In some experiments the complete assembly was immersed in silicone oil (Edwards Vacuum MS705).

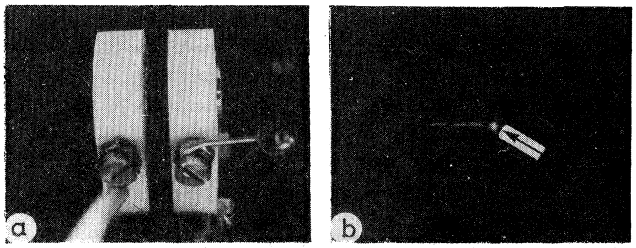

FIG. 3. One-contact experiment. (a) shows the arrangement of the PTFE disks 3.3 mm apart, each having a brass cylinder fitted along its axis. The electrical contacts are made at the screws shown on the disks. (b) shows a AgN_3 crystal (1.35 mm long) supporting a corona discharge (arrowed) without dielectric breakdown. The estimated field in the crystal is ~ 300 kV/m.

If edge effects are ignored, and the system is regarded as two lossless capacitors in series, an assumption that should be sufficiently valid until a large discharge current passes through the sample to the opposite cylinder, the field supported by the crystal may then be estimated as

$$F=\epsilon'\phi/(\epsilon' l+\epsilon l') \,. \tag{8}$$

Here, ϕ is the voltage across the cylinders, ϵ' represents the static relative permittivity of the ambient and is ~ 1 for air or 2 for oil, l is the length of the crystal (the dielectric constant of which is $\epsilon=9.5$), and l' is defined by $l+l'\equiv$ distance between cylinders. In each experiment the sample was observed visually, while ϕ was increased gradually until particular values of F were reached.

IV. RESULTS

A. Microscopies

We found that the application of an ac field of 43 kV/m peak-to-peak magnitude, but of a frequency greater than 10 Hz, did not produce any changes in the appearance of fresh crystals even after over 20 h. Under the action of a dc field of less than 13 kV/m, giving a current density of less than 1 mA/m^2, crystals similarly remained unchanged for over 3 d.

On the other hand, when the dc field was stronger, so that the current exhibited fluctuations, small opaque globules, which were initially separate from either electrode and from one another, started to appear on the crystal

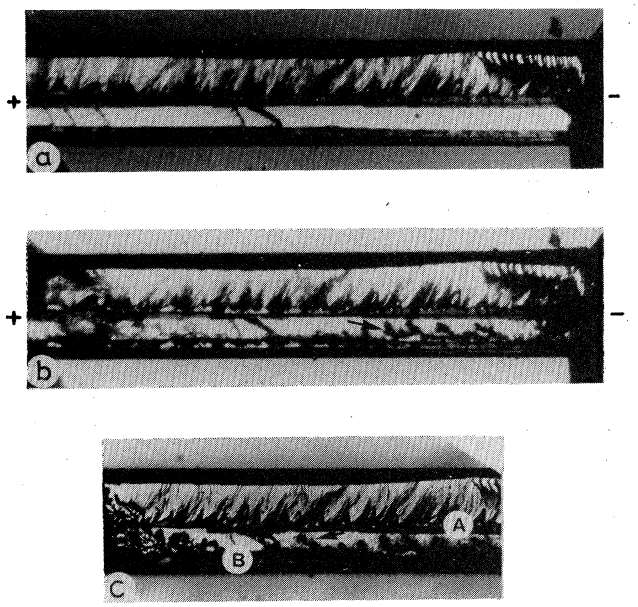

FIG. 4. Slow electrical decomposition in a AgN_3 crystal. Electrodes are of carbon dag and the distance between them is 0.7 mm. The sample is shown at (a) 0, (b) 5, and (c) 30 min after the application of 129 kV/m fields. Arrows in (b) and (c) point to regions where new features have been formed. (c) shows only a part of the crystal, but the magnification is the same as in (a). The formations at *A* and *B* in (c) are shown in Fig. 5 at higher magnifications.

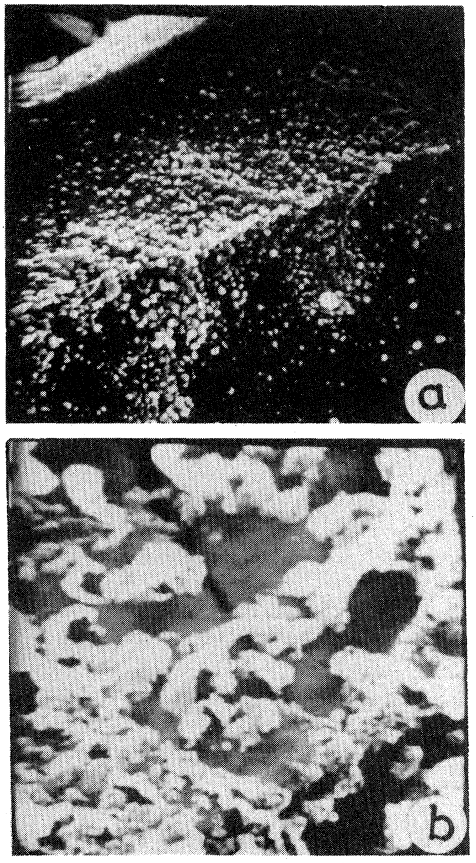

FIG. 5. Scanning electron micrographs of surface formations shown in (c) of Fig. 4. (a) is from region *A*, (b) is from *B*. The widths of (a) and (b) are 75 and 30 μm, respectively. These deposits have been identified as metallic silver.

surface. The number of globules grew with time to give overall "treelike" or dendritic formations at a rate that was higher for a stronger applied field. As an example, in a field of 33 kV/m a crystal exhibited, after about 5 h, new surface features visible under the optical microscope. Upon irradiation of the central part of the crystal by a low-power He-Ne laser (photon energy 1.96 eV), pronounced photoconductivity was observed. This phenomenon is consistent with the presence of metallic silver on the surface: The azide has a band gap of (4.1 ± 0.2) eV and is therefore transparent to the beam, whereas the Schottky barrier between it and silver takes a calculated value of (1.1 ± 0.3) eV.[2] Energy-dispersive x-ray analysis in a Cambridge S4-10 microscope confirmed that the globules contained silver and, being stable in the electron beam, could not be silver azide. Electron-diffraction investigations performed later indicated the development, in earlier stages of electrical decomposition, of (i) clusters of silver atoms having a preferred crystallographic orientation and, subsequently, (ii) micrometer-sized linear structures formed by their accretion.[9]

In general, the distribution of the globules depended little on their positions relative to the electrodes. Indeed, if the polarities of the electrodes were interchanged, as was done for a few samples, the directions and positions of the growth of the "trees" seemed unaffected. This feature shows that the form of decomposition is not electrolysis.

An illustrative case is presented in Fig. 4. An undecomposed crystal of silver azide is shown in Fig. 4(a). A dc field of 129 kV/m was applied through a current-limiting resistor for 5 min; the ensuing changes are depicted in Fig. 4(b); the field was further applied for 25 min and Fig. 4(c) shows the additional changes. Scanning electron micrographs of the surface features are presented in Fig. 5, where the treelike formations are resolved into clusters of globules that protrude from the surface.

An approximate visual estimate of the rate of silver formation suggested that it decreased dramatically after the crystal had been extensively covered with silver. More quantitative results are reported below.

B. Mass spectrometry

It has previously been reported that, under the action of a field "amounting to about 50% of the breakdown strength," a silver azide crystal placed in paraffin oil was seen to give off gas bubbles. These bubbles were distributed throughout the length of the sample.[10] Our mass-spectrometric measurements confirmed that the gas evolved was nitrogen, and that, more precisely, the process took place in the presence of a medium or strong field that led to a fluctuating current. Furthermore, two features were observed. When the average value of the current $i(t)$ increased with time t, the rate of nitrogen

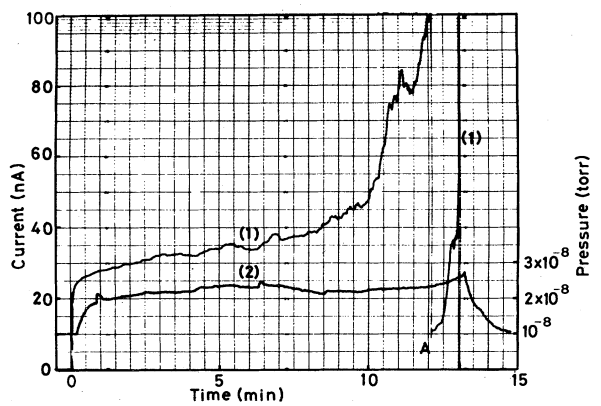

FIG. 6. Electrical decomposition of a single crystal of AgN_3 monitored with a mass spectrometer. Here the isolation valve between the pump and the experimental chamber was only partially closed. Trace (1) represents the conduction current through the crystal, whereas trace (2) gives the partial pressure of nitrogen in the chamber. At A [trace (1)] the current sensitivity of the recorder was decreased by a factor of 10. The rate of nitrogen evolution, d, has been calculated from the recorded partial pressure p with the time constant τ of the system taking the measured value of (26±5) s [see Eqs. (6) and (7)]. The sample dimensions were (280×290) μm×3.0 mm. It was subjected to 400 V dc. Note that pressure trace (2) is slightly displaced to the right on the time axis because of instrumental necessity.

generation $d(t)$ remained more or less constant, and only began to rise after $i(t)$ approached a thousandth of its breakdown magnitude. Second, there were short bursts of nitrogen evolution superimposed on the constant-rate evolution process. Both of these characteristics are apparent in Fig. 6. We found that a crystal, when subjected to 40-kV/m peak-to-peak ac fields of frequencies greater than 10 Hz, did not produce nitrogen at any detectable rate.

Figure 7 is based on a quantitative analysis of the data from three crystals. One was studied in the mass spectrometer with the valve closed. For the other two, the pump was only partially isolated; their data have been processed according to Eq. (7). The ratio of d to $i(0)/q$, where q is the electronic charge, appears to be 0.3 universally.

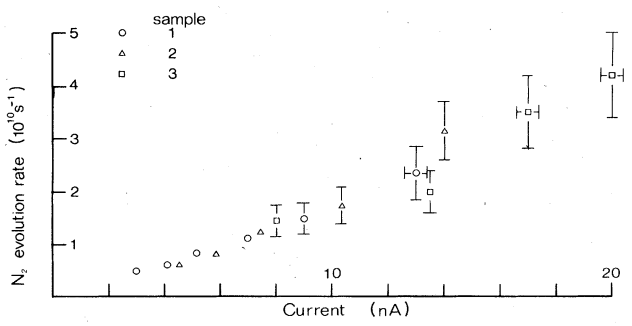

FIG. 7. Initial rate of nitrogen evolution as a function of the magnitude of the initial current. Each measurement corresponds to a particular value of the applied field.

C. Memory effect

It was observed that if a dc field of strength greater than the critical value of 13 kV/m was applied for a period of time and then turned off, and this sequence repeated several times, the current-time response was different each time, although right at the start of each application the magnitude of the current was always the same. On the other hand, the rate of increase of conduction current increased with the sequential number of the application of the field. Results from a typical experiment are shown in Fig. 8. Traces (1)—(3) represent the conduction current when the field of the same magnitude was applied and then switched off, repeating the sequence three times; the first application was for just under 2 min, while the remaining two were for shorter periods. Trace (4) represents the pressure of the evolved nitrogen gas. Note that the rate of rise of the partial pressure is controlled by the time constant of the vacuum system [see Eqs. (6) and (7)] and the rate of evolution of nitrogen from the crystal, the latter being constant for a given applied field.

D. Fast-decomposition initiation

The characteristic pattern of the explosion residue is illustrated in Fig. 9(a). "Flow lines" converge along the direction in which explosion propagated. A point at which the flow lines change their orientation is therefore a location where explosion initiated. Figure 9(b) shows the residue left by a crystal in which initiation occurred at two separate locations, one of which, in this particular case, is near the crystal-cathode interface.

Eight samples with carbon-dag electrodes were examined. In four of them individual explosions were deduced

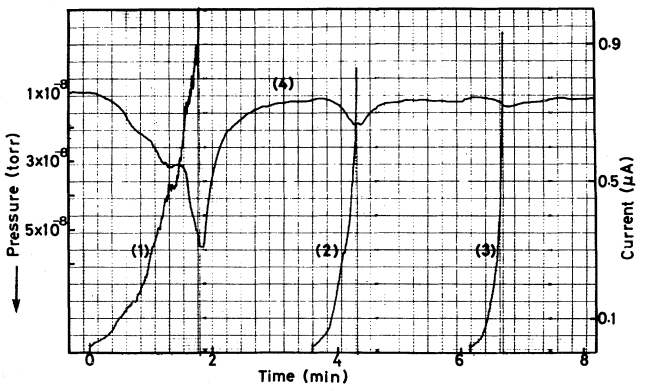

FIG. 8. Manifestation of the "memory effect" by a silver azide crystal of dimensions (280×290) μm×3.0 mm. 400 V dc was applied for short periods of time (as shown) across the length of the crystal in an ultrahigh-vacuum system in which the isolation valve between the experimental chamber and the vacuum pump was only partially closed. The conduction current is shown by traces (1)—(3), whereas trace (4) represents the partial pressure of the evolved nitrogen gas. Note that the rate of rise of the conduction current increases with the sequential number of the field application. On the other hand, the rate of rise of the partial pressure is controlled by the time constant of the system [see Eqs. (6) and (7)] and the rate of evolution of nitrogen, which is constant at a given field.

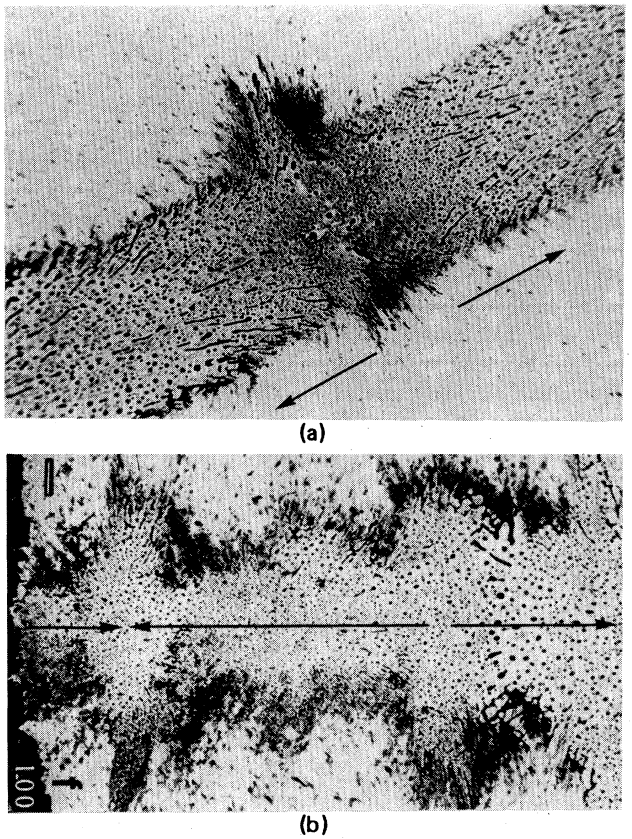

FIG. 9. Residues left on glass slides after explosions of AgN_3 crystals due to the application of an electric field. (a) 180 kV/m through carbon-dag electrodes; (b) 250 kV/m through silver-dag electrodes. The dark band to the left of (b) is the cathode. Arrows indicate the deduced direction of the propagation of the explosion. Width of (a), 2.1 mm; width of (b), 1.7 mm.

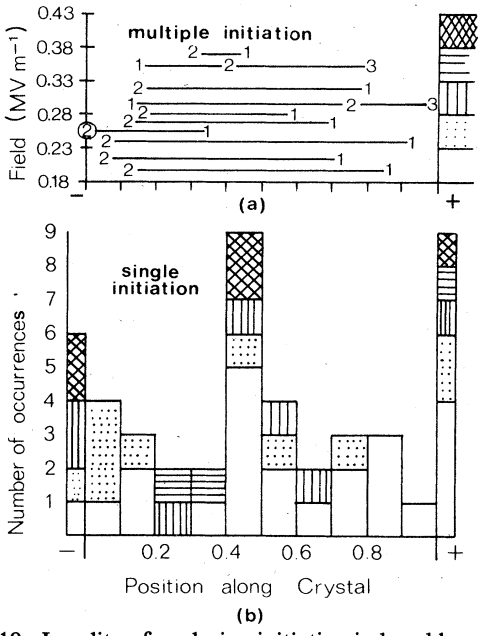

FIG. 10. Locality of explosion initiation induced by a dc field applied through silver-dag electrodes. The statistics for multiple initiation in a single specimen is presented in (a), and that for single initiation is given in (b). The interelectrode distance is normalized to 1; cathode is shown as − and the anode as +. In (a) the deduced sequence of multiple initiation in a single sample is represented by digits 1—3; initiation first occurs at the normalized positon 1 followed by initiation at 2 and 3, in that order. In (b) the different shadings of the area under the histogram indicate the ranges for the individual magnitudes of the applied fields as defined in (a).

to have been initiated around the middle section—one near the cathode and three at the anode-crystal interface. The results in the case of silver-dag electrodes are summarized more quantitatively in Fig. 10. Out of 58 samples, eight had two initiation sites and two had three initiation sites each; the rest had one. In four of them, individual explosions were deduced to have been initiated around the middle section. The salient feature in all cases is that the initiation of an explosion can generally occur away from either electrode.

High-speed photographic sequences confirmed the same feature. An example is shown in Fig. 11. The sites of location are apparent, as spherical shock fronts produced in the oil surrounding the crystal appear dark in the backlit photographs.

E. One-contact experiments

It was found that for a crystal in contact with only one electrode an intense dc field of either sign could be withstood without an explosion being initiated. With the experimental assembly in air, corona discharge occurred at the free end of the sample when the voltage between the electrodes, ϕ, exceeded about 6 kV. The discharge, blue in color, could be seen with the naked eye or photographed [see Fig. 3(b)]. Its size increased with ϕ and occasionally a few glow spots were also noticed on the surface of the brass cylinder opposite the free end. After sustaining the discharge for several minutes, the crystal was found to be blackened at this end, and, when dipped into a weak ammonia solution which dissolved silver azide slowly, a thin

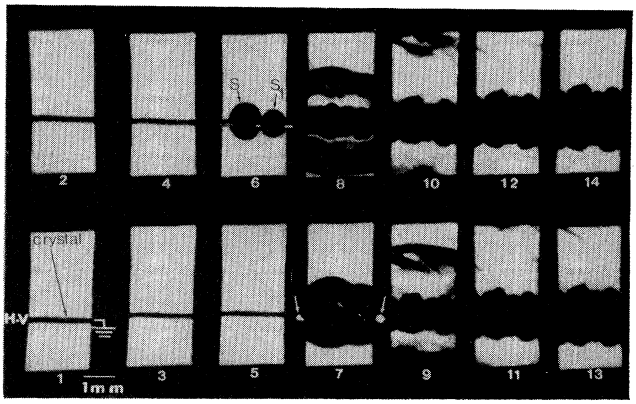

FIG. 11. High-speed photographic sequence of the initiation of an explosion in a single crystal of AgN_3 by the application of a dc field of 10 MV/m. The field, applied between frames 2 and 3, reached the maximum value in frame 5. Initiation took place at the two locations marked S and S_1 in frame 6. Interframe time, 0.2 μs.

brownish film floated off, leaving the tip transparent once again. The blackening obviously represented surface decomposition. For each of the cases examined, the field in the sample, F, was estimated at 250 to 350 kV/m according to Eq. (8). F therefore approached the 1-s, 50% value listed in Table I. Nevertheless, the decomposition caused was always not only much less than that in the case of two conducting contacts (see Sec. III A), but also different in kind, being confined to the tip [cf. Fig. 3(b)]. We interpret it as simply decomposition due to the heating, uv irradiation, or the impact of charged particles generated by the corona. Further support for this view comes from other experiments in which the entire assembly was immersed in silicone oil. No explosion occurred after 5 min for F as high as 1 MV/m, and subsequent examination under an optical microscope revealed no decomposition.

These observations established a necessary condition for electrical decomposition, namely the presence of conducting contacts. The mechanism to be put forward below is consistent with this fact.

V. DISCUSSION

Our work has established that the lowest dc-field strength of silver azide at room temperature that can cause dielectric breakdown is 13 kV/m, which is some 4 orders of magnitude smaller than that for most other ionic solids, and that the delay time to breakdown may be up to days. Such characteristics suggest that the phenomenon under study is qualitatively different from either a thermal or an electronic avalanche-type breakdown. We propose here a mechanism for the phenomenon in which two distinct stages are recognized, namely electrical decomposition and then thermal decomposition. For the sake of clarity, the discussion that follows will be grouped under different aspects of the two successive stages.

A. Current instabilities

The results from the various series of experiments described in Sec. IV have shown that under an applied dc field of strength greater than the critical value a crystal decomposes only when the current through it develops instabilities. Furthermore, if the field across the crystal is applied in a manner such that the contact is made only at one of the ends, no decomposition occurs even for relatively strong fields. There is no decomposition when the sample is subjected to relatively high-frequency ac fields.

As the process of decomposition of silver azide requires the generation of free electrons in its conduction band,[2] the current instabilities may be considered to represent the injection of electrons and holes into the silver azide from the cathode and anode, respectively. The injection processes themselves take place because of the existence of intense interfacial space-charge fields due to electrode polarization, which, in turn, is due to the drift of interstitial Ag^+ ions under the action of a dc field applied through partially blocking electrodes. The interfacial space charges are formed since the transport rate of the ions in the crystal exceeds their discharge rate at the cathode.

The presence of the space-charge fields has recently been confirmed by Robinson.[11] He established, using complex impedance data from silver azide samples having thin-silver-film electrodes, that the total thickness of the accumulation and depletion space-charge regions near both electrodes is about 2 nm, and that the fields across these regions are some 2 orders of magnitude greater than the bulk value. Robinson's measurements were made for bulk fields of magnitude less than 1.5 kV/m. We expect that at higher applied fields the interfacial-field enhancement would be greater. Thus for the case of the bulk applied field being critical (i.e., 13 kV/m, the interfacial fields could be in excess of 1 MV/m; at these values the injection of charge carriers from the electrodes into the sample becomes significant.

B. Electrical decomposition

The decomposition of a crystal of silver azide into which electrons and holes are injected can be explained in the following way. Silver azide decomposes exothermically, and it is energetically more favorable for a hole to combine with another than for it to recombine with a free electron. Hole combination represented by

$$N_3^0 + N_3^0 \rightarrow 3N_2\uparrow$$

releases (9.5 ± 0.5) eV of energy, which is greater than twice the band-gap value[2] of (4.1 ± 0.2) eV. Since according to Thomas and Tompkins[12] the activation energy for combination is less than 0.2 eV, the process is kinetically acceptable.

Unlike a hole, a conduction-band electron (e) should have a high mobility. Hence it is kinetically more favorable for the process of the formation of a Ag atom to proceed via the localization of e at a trap at which a silver interstitial ion that is passing by can be discharged. The formation therefore takes place throughout the length of the crystal, not necessarily adjacent to the cathode, at sites where injected electrons, in their drift toward the anode, become localized at traps. In particular, silver atoms on the surface, where there is room for growth, can accrete more atoms by acting as electron traps:

$$Ag_n + e^- \rightleftarrows Ag_n^-, \quad Ag_n^- + Ag^+ \rightleftarrows Ag_{n+1} .$$

The Fermi level of bulk silver has been estimated to be about 2.8 eV below the bottom edge of the conduction band in silver azide.[2] Assuming that small clusters of silver atoms have similar electron energy levels as those in bulk silver, the former can act as electron traps of long lifetimes.

Our model explains the surface distribution of silver formations as observed with microscopy. The underlying mechanism is similar to that suggested previously for the thermal decomposition of silver azide:[2] The only difference lies in the process responsible for the generation of electrons and holes, which is thermal excitation in the thermal case,[2] but field injection in the electrical case.

C. Memory effect

The data from mass-spectrometry experiments indicate a proportionality of the electrical decomposition rate to the initial magnitude of the conduction current. However, for a given applied field the decomposition rate stays the same, whereas the magnitude of the current increases with time. This observation suggests that the new component of the current has a different origin.

Our interpretation is that the additional current is electronic and is carried by surface filaments and islands of metallic silver produced by electrical decomposition (silver filaments, assumed to be formed by electrolysis, have been inferred to exist in silver chloride, the switching action of which has been related to their thermal annealing,[13] i.e., coalescence of metallic clusters and breaking of the filaments). In the case of the electrical decomposition of silver azide, any filament annealing occurs along with silver production. As both processes continue, the base current increases since the dimensions and the number density of the silver islands grow.[14]

In regard to the memory effect (see Sec. IV), when the field is removed the continuity and the arrangement of the filamentary networks and islands, respectively, are likely to be disturbed, the degree of disturbance increasing with the time for which the sample has no applied field across it. On the reapplication of the field only the ionic and field-injected electronic components of the current flow initially; the contribution from the other electronic component comes later as the filament networks and silver islands rearrange under the action of the field.

D. Thermal decomposition and final disruption

In silver azide, Joule heating in the metallic filaments causes not only their annealing but also the thermal decomposition of silver azide. As the heating is proportional to the current density, the maximum temperature rise will be at the thinnest parts of the filaments. These regions of high temperature can give rise to two effects: (i) breakage of the filament with the cessation of the thermal decomposition at the breakage site, and (ii) the filament does not break but the exothermic decomposition results in local self-heating and initiation of fast decomposition which then spreads throughout the sample, thus causing a catastrophic disruption.

This scenario explains the distributed character of initiation sites, and the observation that occasionally there are more than one site on one sample. This model is also consistent with the variation, within relatively wide margins, of the time elapsed before explosion.

VI. CONCLUSIONS

A detailed mechanism for the dielectric breakdown of silver azide has been proposed. The distinguishing aspects of the breakdown phenomenon have been identified as (i) relatively low applied fields at which it can happen, (ii) the long delay times between the application of the field and the breakdown during which fluctuating currents develop, (iii) formation of metallic particles on the surface, and (iv) the exhibition of the memory effect. All these unusual features have been qualitatively explained by our model, according to which electrons and holes injected from polarized electrodes cause chemical decomposition throughout the length of the specimen.

The original model of Bowden and McLaren[4] has been shown to be incompatible with experiments. The possibility of decomposition due to field-assisted defect generation in the bulk, analogous to the dehydroxylation of $Mg(OH)_2$, $Al(OH)_3$, and kaolinite under the joint action of heat and electric field,[15] may safely be ruled out on account of the relatively low field encountered in the bulk. Likewise, it is unnecessary to consider the field ionization of shallow electron levels associated with impurities, which arguably takes place in CdF_2,[16] because in that case the mechanism would still be effected when an ac field is applied.[17]

Preliminary work has pointed to the operation of the postulated mechanism in the ionic azides of thallium and lead[14] as well. The mechanism is, of course, inapplicable to covalent azides, which may be the reason why the latter are more stable under a dc field. Other classes of materials in which bulk electric decomposition seems to result from charge-carrier injection include sodium β-alumina:[18] This superionic solid, when used in a battery, suffers degradation during the charging cycle. Another plausible candidate is CdF_2. This insulator, which becomes superionic at elevated temperatures, conducts by mobile F^- species.[19] It has been reported that, in samples having sputtered gold electrodes, subsurface particles of cadmium metal are formed in the bulk[20] at room temperature, and that polarization of the electrodes occurs, causing the injection of electrons and possibly holes[21] (which when trapped can combine with interstitial anions).

Finally, the proposed mechanism of electrical decomposition may be of relevance to the studies of thermal decomposition of solids placed in an electric field. This research area continues to be active as is illustrated by a study on potassium azide.[22] For some materials, the observed decomposition is probably a composite, part thermal and the rest electrical in nature. If this possibility is not realized, then misleading conclusions may be drawn.[23]

ACKNOWLEDGMENTS

We would like to thank Dr. A. D. Yoffe and Dr. J. E. Field for discussions. This work was supported in part by the Ministry of Defence (Procurement Executive) and in part by the U.S. Government through its European Research Office.

*Present address: Division of Solid-State Chemistry, Institute for Molecular Science, Myodaiji, Okazaki 444, Japan.

[1]K. L. Tsand, Y. Chen, and J. J. O'Dwyer, Phys. Rev. B **26**, 6909 (1982).

[2]T. B. Tang and M. M. Chaudhri, Proc. R. Soc. London, Ser. A **369**, 83 (1979).

[3]M. M. Chaudhri and J. E. Field, J. Solid State Chem. **12**, 72 (1975).

[4]F. P. Bowden and A. C. McLaren, Proc. R. Soc. London, Ser. A **246**, 197 (1958).
[5]D. A. Young, Br. J. Appl. Phys. **15**, 499 (1964).
[6]Yu A. Zakharov, G. G. Savelev, V. V. Boldyrev, and L. A. Votinova, Kinet. Katal. **5**, 709 (1964).
[7]Yu. A. Zakharov and Yu. N. Sukhushin, Izv. Tomsk. Politekh. Inst. **251**, 213 (1970).
[8]A. D. Yoffe, in *Developments in Inorganic Nitrogen Chemistry,* edited by C. B. Colburn (Elsevier, Amsterdam, 1966), Vol. I, p. 72.
[9]C. J. Robinson and M. M. Chaudhri, in *Proceedings of the 1st International Conference on the Conduction and Breakdown in Solid Dielectrics* (IEEE, New York, 1983), p. 322.
[10]Yu. N. Sukhushin, Yu. A. Zakharov, and F. I. Ivanov, Khim Vys. Energ. **7**, 231 (1973) [High Energy Chem. **7**, 261 (1973)].
[11]C. J. Robinson, Ph.D. thesis, University of Cambridge, 1981.
[12]J. G. N. Thomas and F. C. Tompkins, Proc. R. Soc. London, Ser. A **210**, 111 (1951).
[13]A. Friedenberg and Y. Shapira, J. Appl. Phys. **54**, 5171 (1983).
[14]T. B. Tang and M. M. Chaudhri, Nature (London) **282**, 54 (1979).
[15]K. J. D. MacKenzie, J. Therm. Anal. **5**, 363 (1973).
[16]V. Dallacasa, C. Paracchini, and G. Schianchi, in *Proceedings of the 1st International Conference on the Conduction and Breakdown in Solid Dielectrics,* Ref. 9, p. 134.
[17]C. Paracchini, Phys. Rev. B **4**, 2342 (1971); **8**, 848 (1973).
[18]T. B. Tang and M. M. Chaudhri, J. Mater. Sci. **17**, 157 (1982).
[19]P. Suptitz, E. Brink, and D. Becker, Phys. Status Solidi B **54**, 713 (1972).
[20]A. Kessler, J. Phys. (Paris) Colloq. Suppl. No. 7, **41**, C6-492 (1980).
[21]A. Kessler, J. Phys. C **14**, 4357 (1981).
[22]A. de Panafieu, B. S. H. Royce, and T. Russell, J. Chem. Phys. **64**, 1473 (1976).
[23]T. B. Tang and V. Krishna Mohan, Nature (London) **303**, 729 (1983).

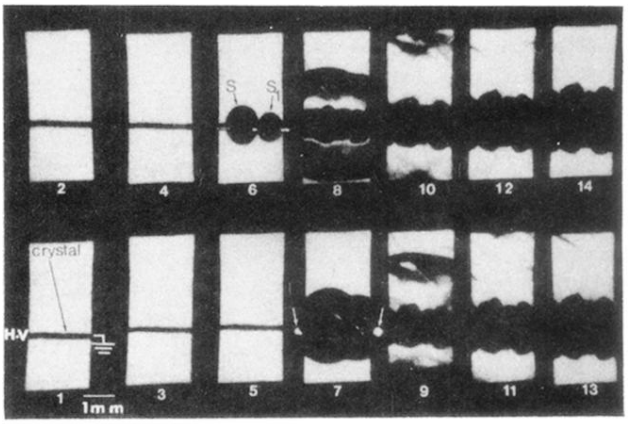

FIG. 11. High-speed photographic sequence of the initiation of an explosion in a single crystal of AgN_3 by the application of a dc field of 10 MV/m. The field, applied between frames 2 and 3, reached the maximum value in frame 5. Initiation took place at the two locations marked S and S_1 in frame 6. Interframe time, 0.2 μs.

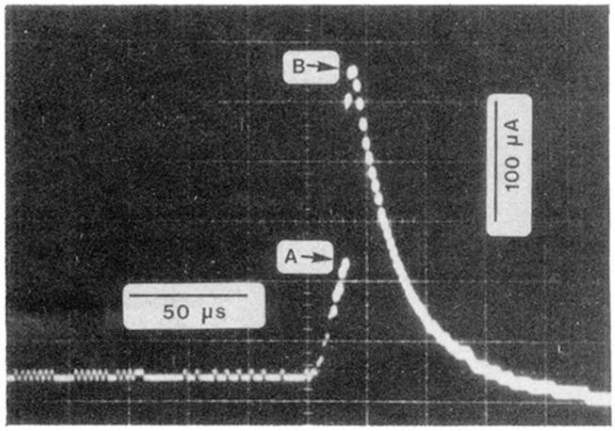

FIG. 2. Current-time behavior of a silver azide single crystal suffering dielectric breakdown. The breakdown at *A* is followed by an explosion at *B*. The decaying current is through the plasma constituted by the explosion products.

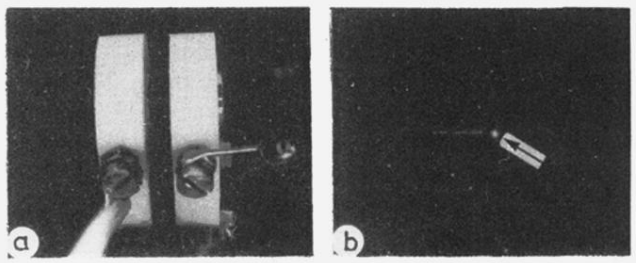

FIG. 3. One-contact experiment. (a) shows the arrangement of the PTFE disks 3.3 mm apart, each having a brass cylinder fitted along its axis. The electrical contacts are made at the screws shown on the disks. (b) shows a AgN_3 crystal (1.35 mm long) supporting a corona discharge (arrowed) without dielectric breakdown. The estimated field in the crystal is ~ 300 kV/m.

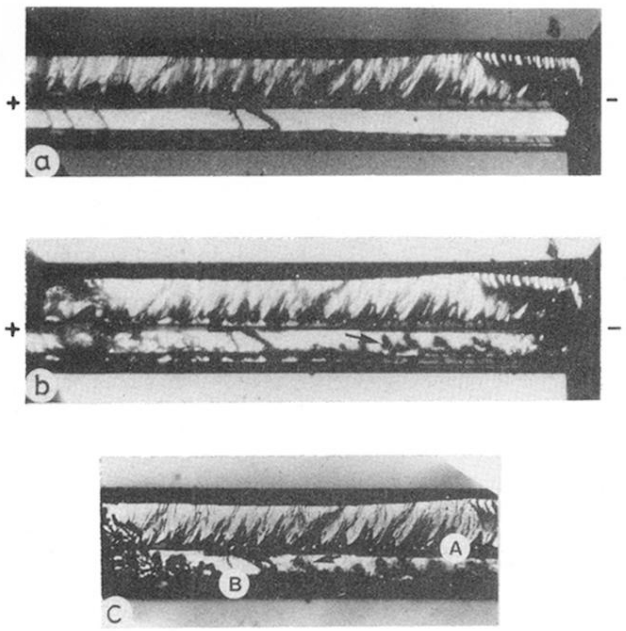

FIG. 4. Slow electrical decomposition in a AgN_3 crystal. Electrodes are of carbon dag and the distance between them is 0.7 mm. The sample is shown at (a) 0, (b) 5, and (c) 30 min after the application of 129 kV/m fields. Arrows in (b) and (c) point to regions where new features have been formed. (c) shows only a part of the crystal, but the magnification is the same as in (a). The formations at *A* and *B* in (c) are shown in Fig. 5 at higher magnifications.

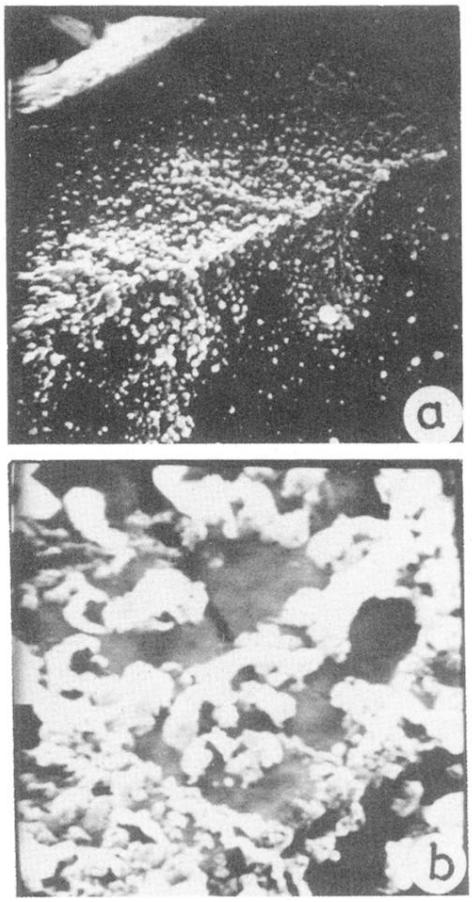

FIG. 5. Scanning electron micrographs of surface formations shown in (c) of Fig. 4. (a) is from region *A*, (b) is from *B*. The widths of (a) and (b) are 75 and 30 μm, respectively. These deposits have been identified as metallic silver.

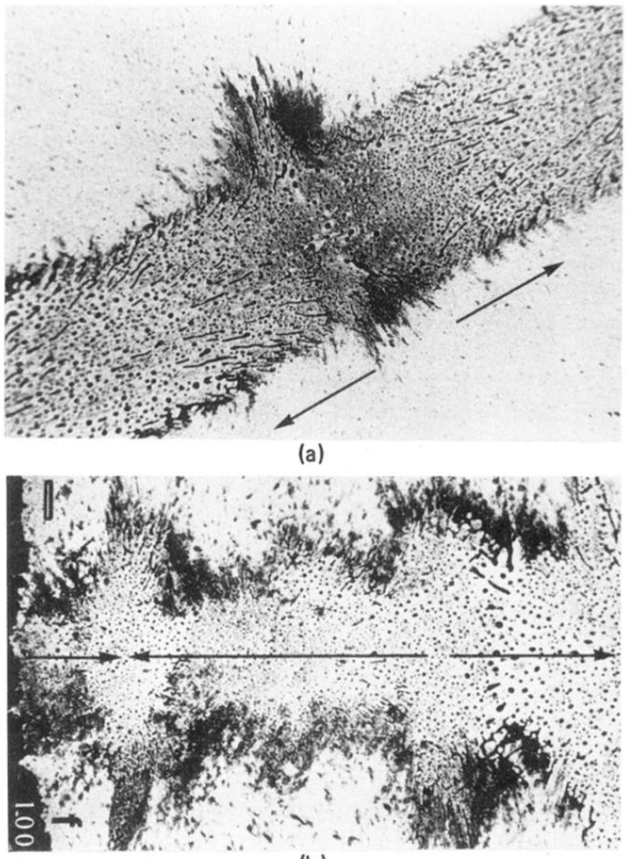

FIG. 9. Residues left on glass slides after explosions of AgN_3 crystals due to the application of an electric field. (a) 180 kV/m through carbon-dag electrodes; (b) 250 kV/m through silver-dag electrodes. The dark band to the left of (b) is the cathode. Arrows indicate the deduced direction of the propagation of the explosion. Width of (a), 2.1 mm; width of (b), 1.7 mm.